Langmuir

Article

pubs.acs.org/Langmuir

Multilayers of Fluorinated Amphiphilic Polyions for Marine Fouling Prevention

Xiaoying Zhu,[†] Shifeng Guo,[†] Dominik Jańczewski,*[,†] Fernando Jose Parra Velandia,[‡] Serena Lay-Ming Teo,[‡] and G. Julius Vancso*[,§,∥]

[†]Institute of Materials Research and Engineering A*STAR (Agency for Science, Technology and Research), 3 Research Link Singapore 117602

[‡]Tropical Marine Science Institute, National University of Singapore, 18 Kent Ridge Road Singapore 119227

[§]Institute of Chemical and Engineering Sciences A*STAR, 1, Pesek Road, Jurong Island, Singapore627833

[∥]MESA+ Institute for Nanotechnology, Materials Science and Technology of Polymers, University of Twente, P.O. Box 217, 7500 AE Enschede, The Netherlands

Supporting Information

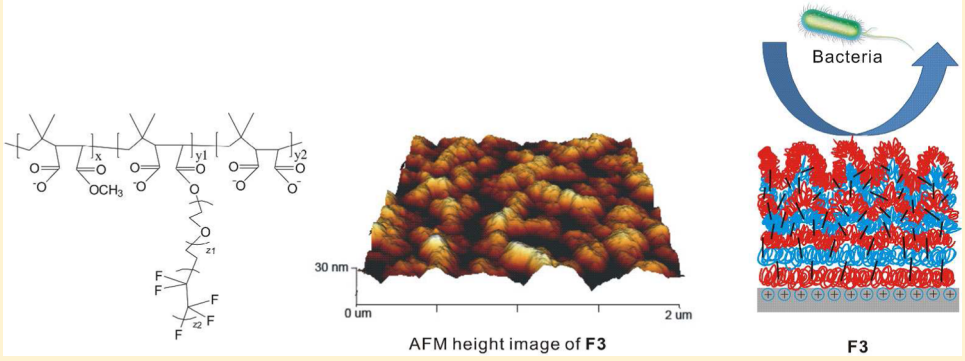

ABSTRACT: Sequential layer-by-layer (LbL) deposition of polyelectrolytes followed by chemical cross-linking was investigated as a method to fabricate functional amphiphilic surfaces for marine biofouling prevention applications. A novel polyanion, grafted with amphiphilic perfluoroalkyl polyethylene glycol (fPEG) side chains, was synthesized and subsequently used to introduce amphiphilic character to the LbL film. The structure of the polyanion was confirmed by FTIR and NMR. Amphiphilicity of the film assembly was demonstrated by both water and hexadecane static contact angles. XPS studies of the cross-linked and annealed amphiphilic LbL films revealed the increased concentration of fPEG content at the film interface. In antifouling assays, the amphiphilic LbL films effectively prevented the adhesion of the marine bacterium *Pseudomonas* (NCIMB 2021).

1. INTRODUCTION

Marine biofouling is the accumulation and growth of micro- and macro-organisms on submerged surfaces in the sea.[1−3] The development of marine biofouling is a dynamic process. The species of organisms in a fouling community and the sequence of attachment or colonization of the foulants are determined by a variety of factors like the substratum, geographical location, the season, and factors such as competition and predation.[1] Biofouling is a serious problem affecting structures critical to the maritime industry such as ship surfaces, harbor installations, oil rigs, underwater sensors, seawater filtration membranes, and pipelines.[4] Various strategies have been proposed to combat marine fouling, and these may be broadly classified into the main trends of biocidal and non or low-adhesive coatings.

Due to environmental issues associated with the use of biocides, low-adhesion coatings have become more popular as the environmentally benign solution. The approaches to prepare low-adhesion surfaces are mainly based on tuning the surface properties[5] such as, topography (or morphology),[6,7] roughness,[8] surface free energy (or wettability)[9,10] and surface charge.[11,12]

It is currently established that hydrophilic surfaces can act as a good antifouling barrier. The hydration layer formed in the vicinity of the hydrophilic coatings should resist nonspecific foulant adsorption.[13,14] For example, a block copolymer comprising polystyrene sulfonate and highly hydrated poly(ethylene glycol)-*graft*-poly(methyl ether acrylate) was synthesized and deposited with polyallylamine hydrochloride to form thin films using the LbL deposition approach providing much better resistance to protein (BSA) and human cancer cell binding.[15] However, once the foulants penetrated the hydration layer, they would firmly attach to the hydrophilic surfaces.[16]

Received: November 6, 2013
Revised: December 9, 2013
Published: December 11, 2013

Hydrophobic, fouling release coatings provide another approach to prevent adhesion of marine organisms. Two families of materials, fluoropolymers and silicones with very low surface free energies, are commonly used to prepare fouling release paints.[17,18] For example, polydimethylsiloxane (PDMS) is widely used in commercial formulations, such as Silastic T-2 from Dow Corning or Intersleek from Akzo Nobel.[19,20] Fluoropolymers have also been shown to be efficient in preventing settlement and removal of fouling organisms such as green alga *Ulva*.[21,22] The low surface free energy of these materials reduces the ability of fouling organisms to adhere to the surface, and shear stress at the surface dislodges any weakly bonded foulers when the vessel is moving.[1,3] However, these hydrophobic fouling release coatings do not prevent foulants from attachment.[1]

Purely hydrophilic or purely hydrophobic surfaces can provide antifouling effects; however, they also have their own disadvantages. The amphiphilic surfaces possessing both hydrophilic and highly hydrophobic domains may overcome these disadvantages by introducing both fouling resistance and release effects. Amphiphilic coatings may also provide dynamic responsive surface with the ability to undergo reconstruction. Diblock[23,24] and triblock[25−28] copolymers with amphiphilic side chains were synthesized by grafting fluorinated molecules with hydrophobic (perfluoroalkyl) and hydrophilic (PEG) blocks to different precursors. The synthesized amphiphilic copolymers were spin coated on the substrates, and in this form have been shown to exhibit better antifouling performances (resistance and enhanced release property) against *Navicula* diatoms and *Ulva* spores than the PDMS based hydrophobic fouling release coatings.[23,27] Hydrophobic perfluoropolyethers cross-linked with a series of hydrophilic PEGs, have been used to prepare a range of amphiphilic networks and applied as marine fouling release coatings[29−31] The commercial amphiphilic surfactant Zonyl FSN-100 (containing ethoxylated fluoroalkyl side chains) can be grafted to polyurethane, and the modified polyurethane can then be deposited onto glass to provide a material with promising fouling resistance and fouling release potential against green alga *Ulva*.[32] Cross-linked hyperbranched fluoropolymers and PEG amphiphilic networks have been shown to achieve good antifouling against marine organisms.[33−35] As many amphiphilic materials have a natural tendency for micelle formation, they often do not display sufficient stability upon deposition on substrates to serve as an effective coating. In such cases, electrostatic LbL assembly could be a convenient, effective and fast method to prepare stable thin polymeric films on various substrates. LbL is carried out by alternating deposition of oppositely charged polyelectrolytes onto the surface.[36] Various functionalized polyelectrolytes, or particles, can be easily immobilized onto the substrate surface by this method.[37,38] However, the fabrication of amphiphilic fluorinated LbL films for marine fouling prevention has not been reported so far.

Thin polymer films obtained by the LbL technique have been used to prevent protein adsorption and bacteria fouling.[15,39,40] However, only a few research papers have reported on the use of LbL assemblies for marine antifouling applications. Our previously reported cross-linked LbL thin film showed high stability and reduced marine fouling.[41] Covalent LbL surfaces prepared by modified PEG and "click" amendable polymers have been demonstrated to have antifouling properties against algae and barnacles.[42] Applying a covalent LbL approach requires, however, specialized sophisticated macromolecules and may not result in a net zero charged film. Electrostatic LbL multilayers consisting of oppositely charged poly(acrylic acid) and PEI after modification with PEG and tridecafluoroctyltriethoxysilane have been used to reduce the attachment of spores of green alga *Ulva*.[43] However, in this case, antifouling was associated with the film roughness achieved in the deposition process, rather than with molecular properties of the LbL film itself. Liu et al. used electrostatically assembled LbL films to produce antifouling coatings, wherein the LbL multilayers served as a scaffold to support superhydrophobic antibacterial system.[44]

In this contribution we investigate LbL fabrication as a way to create amphiphilic surfaces for marine antifouling applications. Our approach is motivated by the possibility to develop a thin film coating with controlled thickness, which could potentially be used in combination with micro topographical patterns.[6,7] Ideally such an amphiphilic coating should display reconstitution of the film surface upon exposure to hydrophobic or hydrophilic environments, but also attain sufficient stability in corrosive seawater. The antifouling activity of the amphiphilic LbL films was evaluated in laboratory tests against two common marine fouling organisms including a marine bacterium (*Pseudomonas*, NCIMB 2021) and a benthic diatom (*Amphora coffeaeformis*). These organisms have been previously used in lab assays to evaluate the antifouling properties of various materials.[42,43,45,46]

2. EXPERIMENTAL SECTION

2.1. Materials and Instruments. Poly(isobutylene-*alt*-maleic anhydride) (PIAMA, M_w: 60 000 D), perfluoroalkyl polyethylene glycol (fPEG, Zonyl FSN-100), polyethylenimine (PEI, M_w: 25 000 D, branched), 3-aminopropyltrimethoxysilane, 4-(dimethylamino)-pyridine (DMAP), and sodium hydroxide were purchased from Sigma Aldrich. Solvents including *N*,*N*-dimethylformamide (DMF), dimethylsulfoxide (DMSO), toluene, methanol, and ethanol were purchased from Tedia. Dialysis membrane tubing (MWCO: 12 000 to 14 000) was received from Fisher Scientific. Silicon wafers were obtained from Latech Scientific Supply Pte. Ltd. Ultrapure water produced by a Millipore Milli-Q integral water purification system was used to prepare aqueous solutions. A triple P plasma processor (Duratek, Taiwan) was used to clean the silicon wafers. NMR (Bruker, 400 MHz), FTIR (Perkin-Elmer) and XPS (VG ESCALAB 250i-XL spectrometer) were used to characterize polymer samples and LbL films.

2.2. Synthesis of the Polyanions P1 and P2. *Polymer P1 Synthesis.* The material was synthesized following the previously published protocol.[41] NMR calculated Mn: 84 kDa. ^{1}H NMR integrated for a single repeating unit: (DMSO) δ_H: 0.92 (6 H, m), 3.52 (0.24 H, s). IR: 1732, 1569, 1473, 1411 cm^{-1}.

Polymer P2 Synthesis. One gram of PIAMA and DMAP (0.026 g) was suspended in 10 mL of DMSO at 65 °C and stirred with 500 rpm magnetic stirrer until the polymer was completely dissolved. Subsequently, 50 μL of methanol was added to the solution to start the reaction. After 5 h, 0.6 g of fPEG was added into the solution. The reaction lasted for another 12 h before pouring into 100 mL of NaOH aqueous solution (10 g/L). When the solution became clear, it was transferred into the dialysis membrane tubing (1 m) and dialyzed against ultrapure water for 3 days. Water used during the process was changed every 12 h. The purified aqueous polymer solution was then concentrated by rotary evaporator and finally freeze-dried to yield the solid polyanion **P2** 1.22 g (yield 76%).

NMR Calculated Mn. 96.5 kDa. ^{1}H NMR integrated for a single repeating unit: (DMSO) δ_H: 0.98 (6 H, m), 3.37−3.78 (4.09 H, m), 4.57 (0.08 H, m), 4.9 (0.1 H, bs). IR: 1732, 1569, 1473, 1411, 1244, 1212, 1147, 1117 cm^{-1}.

2.3. Assembly of the LbL Films. Silicon wafers were cut into 2 cm ×2 cm slides using a DISCO dicing machine (DAD 321). After

dx.doi.org/10.1021/la404300r | *Langmuir* 2014, 30, 288−296

Scheme 1. The Synthesis of Polymers P1 and P2[a]

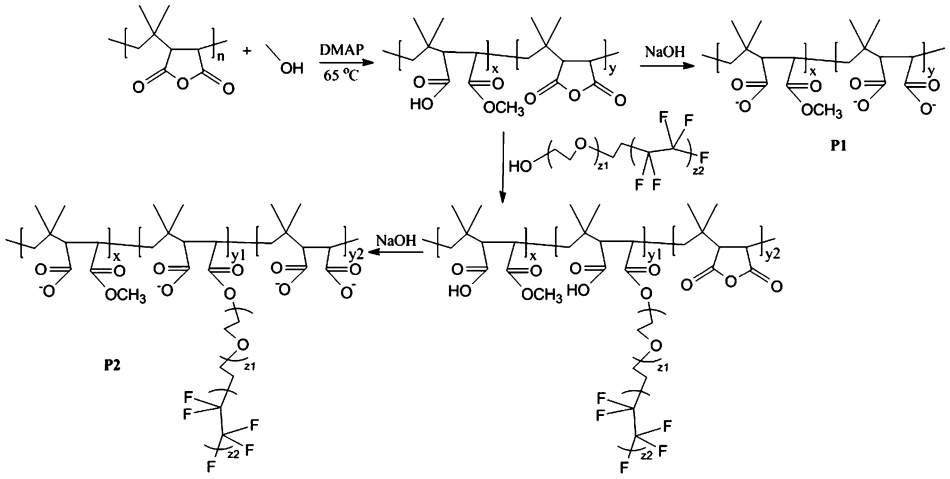

[a] n = 390 (based on the supplier specification), x = 30, y = 360, $y1$ = 15, $y2$ = 345 (calculated from ^{1}H NMR), $z1$ = 5, $z2$ = 4 (refs 24 and 51).

ultrasonic cleaning with water and ethanol for 10 min, the slides were dried over a nitrogen gas stream and treated by oxygen plasma (200 W) for 2 min. The treated silicon wafers were immersed into the 3-aminopropyltrimethoxysilane toluene solution (10 mM) for 5 h to impart positively charged amine groups on the substrate surface.

The pretreated silicon wafer slides were immersed into the aqueous polyanion solution (1 mg/mL) prepared from **P1** or **P2** for 10 min and rinsed with ultrapure water for 2 min. Subsequently, slides were immersed into PEI aqueous solution (1 mg/mL) for 10 min, followed by another 2 min ultrapure water rinse. The cycle was repeated until the desired bilayer number was reached. The silicon wafers with the deposited LbL films were dried by nitrogen stream and later under vacuum at room temperature for 5 h. The cross-linking process was conducted by heating the silicon wafers with the dried LbL films to 60 °C for 5 h under vacuum. The film prepared from **P1** and PEI with 6 bilayers after cross-linking was denoted as **F1**. The films prepared form **P2** and PEI with 5.5 bilayers before and after cross-linking were denoted as **F2** and **F3**, respectively. The prepared LbL films were stored in desiccator for further use.

2.4. Characterization of the LbL Films. The deposited LbL films were analyzed by FTIR and X-ray photoelectron spectroscopy (XPS). The FTIR measurements were collected with a Perkin-Elmer FTIR spectrometer with the Attenuated Total Reflection (ATR) technique using a ZeSe crystal. The XPS spectra of the deposited LbL films were obtained with a VG ESCALAB 250i-XL spectrometer using an Al Kα X-ray source (1486.6 eV photons). The XPS data processing, including peak assignment and peak fitting (fitting algorithm: Simplex), was done by Thermo Avantage v4.12 (Thermo Fisher Scientific). Surface morphology and thickness of the deposited LbL films were measured by a JPK, NanoWizard 3 NanoOptics atomic force microscope (AFM) system in a AC mode (tapping mode). In AFM measurements, Tap300AI-G cantilevers made by Budget Sensors were used. AFM images were taken on dried films over scan size of 2 μm × 2 μm for morphology observations and roughness measurements. The film thickness was measured by scratching the multilayer assembly with a fresh razor blade to expose the bare substrate (silicon) and then scanning the sample over 10 μm × 10 μm to reveal a clear step obtained by the scratch.[47] The height difference between the thin film surface and the bare substrate was considered as the thickness of the thin film. Five sections crossing the step of a single scratch were used to measure the height differences. The mean value of the height differences was calculated as the film thickness. The AFM raw data were processed by software (JPK Data Processing, 4.3.25).

The surface wetting properties of the deposited LbL films were evaluated by contact angle measurements with different liquids including water and oil (hexadecane). A goniometer (250-F1) from Ramé-Hart Instrument Co. was used to measure the contact angles using the static sessile drop method. The silicon wafers with the LbL films were mounted on a flat holder. A 5 μL droplet of water or hexadecane (oil) was dropped onto the dry sample surface through the microsyringe of the device. The liquid droplet image was captured and analyzed by the instrument to obtain the contact angle value of the tested surface. For each sample, 10 measurements of water or oil contact angle at different locations on the LbL film surface were made, and the average value of the measurements was used as the representative water or oil contact angle of the tested LbL film.

The dynamic contact angles were measured by the add−remove volume method using goniometer (250-F1) equipped with an automatic liquid dispenser. After dropping a 5 μL droplet of liquid onto the dry sample surfaces, the advancing (θ_A) and receding contact (θ_R) angles were measured by increasing and decreasing the volume of the liquid drop through the needle of the automatic dispenser while the needle was kept within the liquid drops.

2.5. Biofouling Tests. *2.5.1. Bacteria Adhesion Assay.* Marine bacterial *Pseudomonas* strain NCIMB 2021 obtained from the National Collection of Marine Bacteria (Sussex, UK), cultured in Marine Broth 2216 solution (37.4 g/L) (Difco) was used for the antibacterial tests.[48]

Silicon wafers with the LbL films were immersed in a suspension of stationary phase *Pseudomonas* (NCIMB 2021) for a time up to 6 days. During the test period, the silicon wafers were transferred to a newly prepared stationary phase bacteria suspension in every 48 h to maintain the viable bacteria concentration. Following 6 days of immersion, the silicon wafers were removed from the suspension and fixed in 3 vol % glutaraldehyde phosphate buffered saline (PBS) solutions for 5 h at 4 °C. After fixing, these silicon wafers were rinsed with PBS to remove remaining glutaraldehyde and then dried at 60 °C in the oven for 24 h. The dried samples were coated with gold and imaged with a scanning electron microscope (SEM, JEOL JSM-5600LV).

The surface coverage of bacteria was estimated by image analysis of the SEM micrographs with the ImageJ program (available as a public domain Java image processing program provided by the National Institute of Health, USA). The total area covered by the bacteria clusters was calculated, and then divided by the total area of the image to give the information on percentage coverage of bacteria on the silicon wafer surface. The bacteria coverage for each sample was calculated based on 10 images of different locations on this sample. Three samples were measured for each type of surfaces to get the average bacteria coverage. Plasma cleaned silicon wafers were also measured as a reference surface for adhesion testing.

2.5.2. Amphora Adhesion Assay. Benthic microalgae, *Amphora coffeaeformis*, is one of the most commonly encountered raphid diatoms found in the biofilms of submerged surfaces, and as such, is often used in antifouling tests.[49] *Amphora coffeaeformis* (UTEX

dx.doi.org/10.1021/la404300r | *Langmuir* 2014, 30, 288−296

Scheme 2. LbL Assembly and Top Layer Surface Reconstruction of the Amphiphilic LbL Film

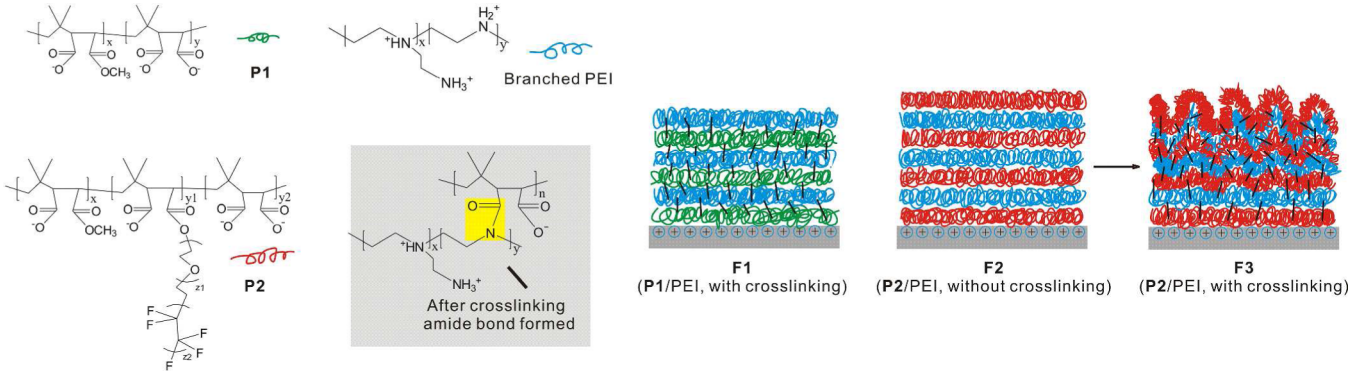

reference number B2080) was maintained in F/2 medium[50] in tissue culture flasks at 24 °C under a 12 h light: 12 h dark regime for at least a week prior to use. In order to be used for the test, the algae cells were gently removed from culture flasks with cell scrapper; subsequently the algae clumps were broken up by continuous pipetting and filtering through a 35 μm nitex mesh. The total number of cells collected per milliliter was determined by using a hemocytometer.

The silicon wafer controls, silicon wafers with LbL films, were placed randomly in six-well Nunc culture plates, one coupon per well, with eight replicates for each treatment, then soaked in 5 mL of 30 ‰ 0.22 μm filtered seawater (FSW) for 12 h prior to use. Next, a load of 50.000 *Amphora* cells (around 350 μL) was added to each well, and all the eight well plates were placed in an environmental chamber with a 12 h light:12 h dark regime at 24 °C and allowed to incubate for at least 24 h under static water condition without any flow. At the end of this period, unattached cells were gently rinsed off with 30 ‰ FSW three times. Slides were subsequently examined under an epifluorescence microscope. Ten random fields of view were scored at 20 times magnifications (0.916 mm^2 per field of view) for each slide.

ANOVA tests followed by *post hoc* Tukey's multiple comparison test (α = 0.05) were used to evaluate the antifouling activity of the amphiphilic LbL films on the numbers of *Amphora* adhered cells per mm^2 as well as to assess whether there were significant variations in these numbers in the presence of surface modification. ANOVA and Tukey's multiple comparison tests were performed by using R (Development Core Team, 2010) software package.

3. RESULTS AND DISCUSSION

3.1. Synthesis of the Amphiphilic and Cross-Linkable Polymer. It has been reported that amphiphilic surfaces may provide enhanced marine antifouling effects including fouling resistance and fouling release.[2] For the fabrication of LbL films with amphiphilic character, a novel polyanion was synthesized through partial alcoholysis of a polyanhydride (PIAMA) with perfluoroalkyl polyethylene glycol (fPEG), (Scheme 1). fPEG was grafted to the PIAMA backbone using hydroxyl group and formation of ester bond with the anhydride group.

Since stability of the LbL films is an important concern, easily cross-linkable methyl esters were introduced via alcoholysis of PIAMA with methanol to promote film cross-linking.[41] Subsequently, the rest of the anhydride groups of PIAMA were hydrolyzed by NaOH as shown in Scheme 1. This process yielded the polymer **P2.** It features amphiphilic side groups, methyl ester groups for cross-linking, and carboxylic groups that provide an anionic character. Charged anionic groups are essential for electrostatic interactions during the LbL assembly. In parallel, PIAMA was directly grafted with methyl esters and hydrolyzed by NaOH to produce the polyanion **P1**, used in this work as a reference.

The polymer structure was verified by both ^{1}H NMR and FTIR. The presence of a peak at 4.57 ppm in the **P2**, but not in the **P1** ^{1}H NMR spectrum, belonging to $C(O)OCH_2$ protons,[52] indicates the formation of the ethyl ester bonds between PIAMA and fPEG. In addition, the peak at 4.90 ppm, in the **P2** but not in the **P1** ^{1}H NMR spectrum, could be assigned to CF_2CH_2 protons further confirming the successful grafting of the fPEG.

From the peak area ratio between the **P2** ethyl ester protons of fPEG at 4.57 ppm, and the methyl group protons from the main chain at around 1 ppm, the percentage of fPEG grafted moiety can be estimated to 4% of the polymer's repeating units. This translates to 5.2% mass of the fluorine.

Based on the peak area ratio between the methyl ester protons and the methyl group protons of the main chain, it can be estimated that about 8% of the polymer's repeating units were bearing methyl esters. The indices *x*, *y*1 and *y*2 describing the composition of **P2** can be estimated to 30, 15 and 345, respectively (Scheme 1).

Additional verification for **P1** and **P2** was provided by FTIR spectra. The double stretching signal ν_{C-F} (1244 cm^{-1} and 1212 cm^{-1}) belonging to CF_2 and CF_3 in the **P2** IR spectrum is not visible in the **P1**, indicating the existence of fluoroalkyl (highly hydrophobic portion) in **P2**.[52] At the same time, double stretching signal ν_{C-O-C} (1118 cm^{-1} and 1147 cm^{-1}) belonging to CH_2-O-CH_2 in the **P2**'s FTIR spectrum is not visible in the **P1**'s, indicating the existence of poly ethylene glycol (PEG, hydrophilic portion) in **P2**.[52] The ester stretching $\nu_{C=O}$ peak at 1733 cm^{-1} and the carboxylic acid stretching peak $\nu_{C=O}$ at around 1571 cm^{-1} are clearly observable for both **P1** and **P2** polymers (see Supporting Information, Figure S3).

3.2. Fabrication and Amphiphilicity of the LbL Films. The newly synthesized polymers **P1** and **P2** were deposited on the silicon substrates using the LbL approach.

The **F2** LbL film was prepared by alternating deposition of the amphiphilic polymer **P2** and PEI. The thickness of the **F2** LbL film with 5.5 bilayers was 77 ± 5 nm. After cross-linking of **F2**, the newly formed film, with the same average thickness of 76 ± 6 nm, was denoted as **F3**. At the same time the **P1** polymer was used with PEI to prepare LbL films (**F1**) for comparison. The thickness of the cross-linked **F1** film with 6 bilayers was 64 ± 3 nm. Amphiphilic block copolymers can form micellar structures in selected solvents.[53,54] According to the dynamic laser scattering (DLS) experiments, both **P1** and **P2** formed micellar aggregates in solution (see Supporting Information, Figure S4). This behavior affected the film

dx.doi.org/10.1021/la404300r | *Langmuir* 2014, 30, 288−296

formation and resulted in relatively high film thickness for both **F1** and **F2**.

The assembly of LbL films is primarily driven by the combination of electrostatic interactions and increase of the entropy during the release of counterions upon assembly.[55] Since seawater is a rather corrosive environment, those forces are considered not sufficient to provide long-term film stability. Hence, covalent cross-linking of polymeric layers was used to improve the stability of the LbL films. In this study, the aminolysis reaction between amine groups of PEI and methyl ester groups of **P1** or **P2** was implemented using protocols described previously.[41] The reaction was verified by the FTIR spectra of the LbL film before and after cross-linking. After the treatment a new peak $\nu_{C=O}$ at 1653 cm^{-1}, belonging to the amide bond stretching frequency, shows up indicating reaction progress. At the same time, the ester stretching signal $\nu_{C=O}$ at 1724 cm^{-1} (see Supporting Information, Figure S5)[52] decreased upon annealing, indicating the consumption of methyl ester groups in **P2**. One product of nucleophilic substitution of **P2**'s methyl ester by the amine groups of PEI is methanol, which can be easily removed under vacuum. By contrast, fPEG, which is the product of nucleophilic substitution of **P2**'s fluorinated chain by amine groups of PEI, cannot be so easily removed from the LbL system in the mild conditions used due to its high vapor pressure. This allows for the selective reaction of methyl ester and preserves fluorinated side chains within the film upon cross-linking. A comparison of FTIR spectrum of ν_{C-F} signals in films before and after cross-linking shows only a small loss of intensity, indicating preserving the majority of the fPEG side groups (see Supporting Information, Figure S5).

3.3. Surface Rearrangement of the Amphiphilic Copolymer during Cross-Linking and Annealing. Surface rearrangement phenomena are well documented for copolymers containing fluorinated blocks.[24,33] This thermodynamically driven process may reorganize the surface chemical composition, topography or morphology of polymeric films.[33] Interestingly, during the segregation process, the amphiphilic brushes may concentrate onto the film surface.[24]

In this study, AFM was used to investigate the morphologies of the LbL films. As shown in Figure 1, the **F1** LbL film exhibited a very low surface roughness (Ra = 0.37 nm). In addition, the phase image of **F1** indicated a homogeneous polymeric surface. The **F2** film also showed a flat surface (Ra = 1.57 nm). After cross-linking and simultaneous annealing, the **F3** film showed a higher roughness (Ra = 4.36 nm). As the AFM image height images show, there is substantial roughening of the multilayers during the annealing and cross-linking process. This roughening takes place at length scales on the order of 20 nm as shown by the height image captured in Figure 1e. Thus the process substantially alters the original LbL morphology (Figure 1).

The fabricated LbL films were characterized by static contact angles of water and hexadecane, measured with the static sessile drop method, and by dynamic water contact angles, measured with the add-remove volume method.

As shown in Table 1, the bare silicon wafer cleaned by oxygen plasma showed the lowest water contact angle at around 15°. However, the silicon wafer surface coated with **F1** had the highest water contact angle at around 71° with low hysteresis of 14°. The **F2** film prepared from **P2** and PEI showed water contact angle value 61° and the water contact angle hysteresis 19°. After cross-linking, the water contact angle of **F3** film decreased to a value around 47°. In addition, the water contact angle hysteresis of **F3** increased to 21°.

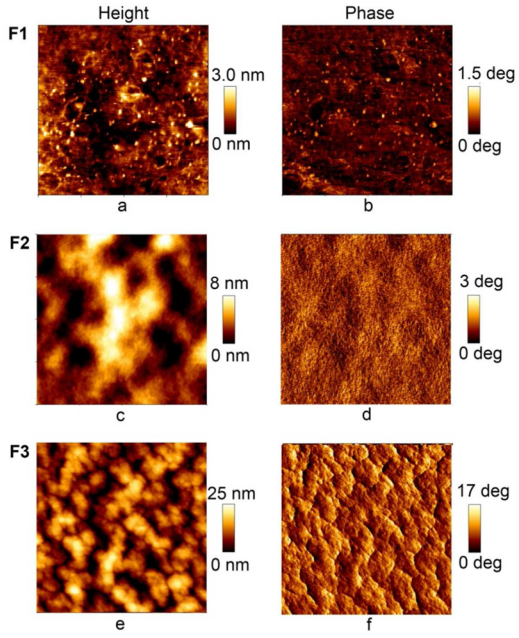

Figure 1. AFM height (left) and phase (right) images (size: 2 μm × 2 μm) of the **F1** (a and b), **F2** (c and d), and **F3** (e and f) LbL films.

Table 1. Static and Dynamic Contact Angles of the Bare Silicon Wafer (Control), and the LbL Films F1, F2, and F3

LbL films	control	F1	F2	F3
water contact angle (deg)	15 ± 3	71 ± 5	61 ± 4	47 ± 2
water advancing contact angle (θ_A, °)	na	74 ± 3	65 ± 1	53 ± 4
water receding contact angle (θ_R, °)	na	61 ± 2	46 ± 3	32 ± 2
water contact angle hysteresis ($\Delta\theta$, °)	na	14	19	21
oil (hexadecane) contact angle (°)	0	0	30 ± 2	41 ± 2

The static water contact angle results indicated that the hydrophilicity of the **F2** LbL film was improved due to the hydrophilic PEG moiety of **P2**. On the other hand, the dynamic water contact angle results indicate a surface reconstruction of the amphiphilic LbL films. The water contact angle hysteresis of **F2** was larger than that of only hydrophobic **F1**. The larger contact angle hysteresis suggests more obvious and faster surface reorganization with changing surface environment.[56] After cross-linking, the affinity of the **F3** film to water was further improved after more obvious surface reconstruction, showing the lowest water receding contact angle and the largest water contact angle hysteresis.

Both the bare silicon wafer and the **F1** LbL film had very low oil contact angles close to 0°. By contrast, the **F2** LbL film showed an oil contact angle value of 30°. The oil contact angle of **F3** was further increased to 41°.

It seems that the existence of **P2** endured the **F2** and **F3** LbL films with hydrophilicity and high hydrophobicity (oleophobicity) at the same time. A similar effect of simultaneous reduction of water contact angle and increase of oil contact angle was also reported for fluorinated amphiphilic brushes.[57,58] On the other hand, the cross-linking process might improve the

dx.doi.org/10.1021/la404300r | *Langmuir* 2014, 30, 288−296

amphiphilicity of the **F3** film showing lower water contact angle and higher oil contact angle than the **F2** film.

Environmentally dependent surface reconstruction by flipping of the amphiphilic side chains could be responsible for amphiphilic surface character. It has been reported that when a surface contacts water, the highly hydrophobic fluoroalkyl chains will bend and the hydrophilic PEG chains are exposed to water to minimize the energy, and display low water contact angle. When the surface is contacting oil or hydrophobic substances (foulants), the highly hydrophobic fluoroalkyl chains will stretch out to minimize the enthalpy, displaying oleophobicity or high hydrophobicity.[23,32]

The surface chemical compositions of the **F1**, **F2**, and **F3** films were also studied with XPS. The fluorine signal is absent in the **F1**'s spectrum. However, a clearly visible fluorine peak can be seen from the XPS spectrum of **F2**. After integration and conversion of the atom percentage to mass percentage, it was found that 1.9% of the mass on the **F2** LbL film top surface is fluorine. The mass percentage of fluorine in the **F3** film top surface layer increased substantially upon cross-linking reaching 7.9%. At the same time, the portion of oxygen on **F3** was also higher than on **F2**. Fluorine and oxygen are the main elements of the fPEG chains, indicating the presence of fPEG moieties on the **F3** film surface. It correlates well with the contact angle measurements and suggests that amphiphilic side chains from **P2** were substantially surface segregated and concentrated on the **F3** film surface.

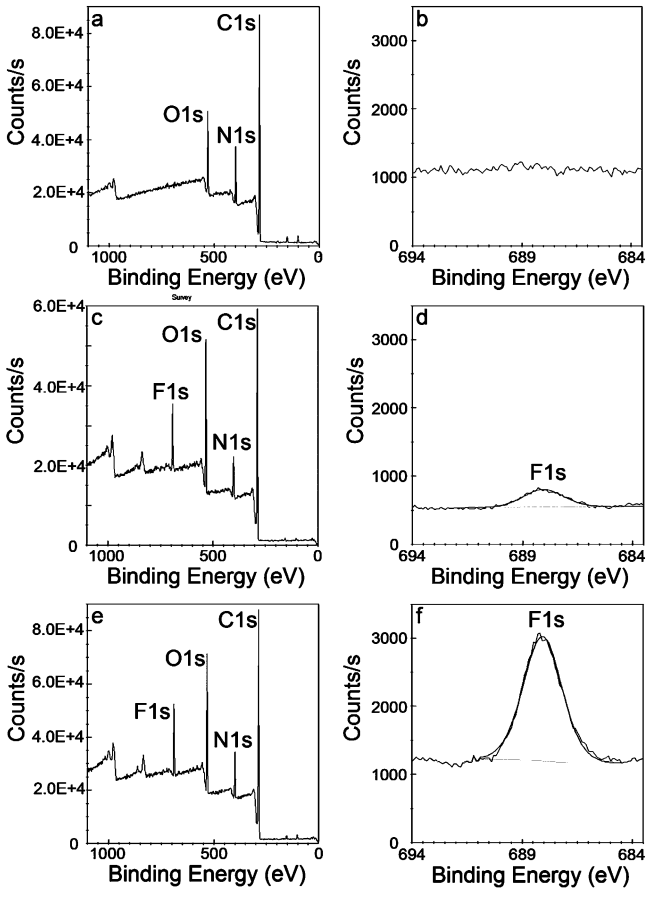

Figure 2. XPS spectra of the LbL films **F1** (a and b), **F2** (c and d), and **F3** (e and f) including full spectrum survey (left) and fluorine atom (1s) scan (right).

Table 2. The mass Percentages of Elements on the Surfaces of LbL Films Based on XPS

	element			
LbL film	C (1s) wt %	N (1s) wt %	O (1s) wt %	F (1s) wt %
F1	72.7%	13.0%	14.3%	0
F2	78.7%	9.6%	9.8%	1.9%
F3	62.1%	9.2%	20.8%	7.9%

3.4. Antifouling Activity of the Surface with the Amphiphilic LbL Film. Antifouling activity of the **F3** LbL film was evaluated against two marine foulants. *Pseudomonas* (NCIMB 2021) is a marine bacterium isolated from marine biofilms. The bacterium is present in most environments, and identified as one of the most common bacteria promoting biofouling, due to its extracellular polysaccharide (EPS) secretions.[59] *Pseudomonas* species have often been used to examine the biofouling formation process.[46,60] In this study, silicon wafers with and without the amphiphilic LbL film (**F3**) were immersed in the bacteria suspension for 6 days and subsequently evaluated for microorganism presence using SEM.

As shown in Figure 3, the bacteria coverage on the bare silicon wafer control was around 38%. However, almost no

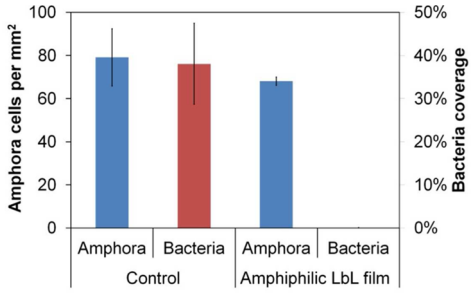

Figure 3. *Amphora* and Bacteria adhesion assays results.

bacteria can be observed on the surface coated with the amphiphilic LbL film (**F3**). Figure 4 shows two examples of the control surface and the surface covered with **F3** after incubation in *Pseudomonas* (NCIMB 2021) for six days. It appears that the **F3** LbL film was able to prevent biofilm formation by *Pseudomonas* (NCIMB 2021) compared to the bare silicon wafer.

Additional tests were carried out with *Amphora coffeaeformis*. After incubation in the *Amphora* suspension, the surfaces were investigated with fluorescence microscopy, and the number of attached *Amphora* cells was scored. As shown in Figure 3, about 79 cells/mm^2 were observed on the control surface (bare silicon wafer) compared to 68 cells/mm^2 observed on the **F3**. Although the difference was not statistically significant, there was lower settlement on the amphiphilic surface than on the control bare silicon surface.

During the film annealing and cross-linking, amphiphilic side chains of **P2**, bearing hydrophilic (PEG) and hydrophobic (fluoroalkyl) blocks, are concentrated near the surface. These two moieties have different contributions in the fouling prevention process. Due to a relatively high surface energy (>43 mJ/m^2) of PEG, PEG containing surfaces have a low interfacial energy with water and form thick hydration layers.[2] As a result, a steric repulsion of the adhesive molecule caused by the hydrated PEG will provide nonspecific resistance to foulants.[21] On the other hand, the CF_3-terminated fluoroalkyl

dx.doi.org/10.1021/la404300r | *Langmuir* 2014, 30, 288−296

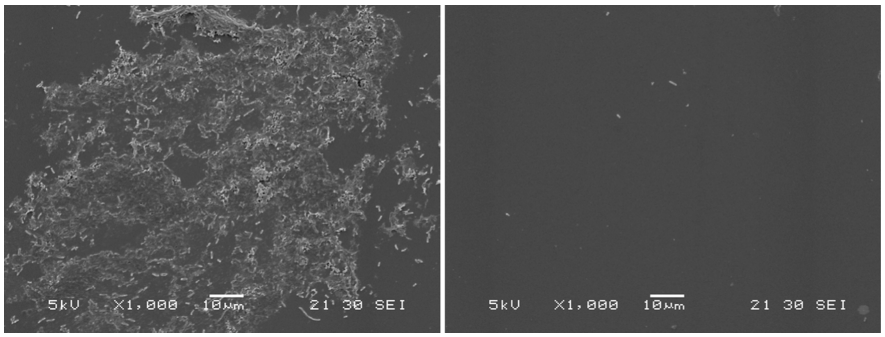

Figure 4. SEM images of the silicon wafer without (left) and with (right) the amphiphilic LbL film (**F3**).

groups have a low surface energy (12−17 mJ/m^2) and thus, the interactions with the foulants are weak and cleavable.[2]

Based on previous reports, we can conclude that the antifouling properties of the amphiphilic surface can be derived from a dual mode of action of film components. The PEG moiety of the **F3** LbL film forms a hydration layer on the film surface to reduce the ability of the marine foulants to contact or attach to the surface. It is likely that, where hydrophobic foulants are able to reach the film, the fluoroalkyl groups would be stretched out, resulting in only a weak interaction between the film and the approaching matter, thus promoting easy detachment of the organism from the surface.

4. CONCLUSIONS

A novel, robust method to fabricate amphiphilic antifouling surfaces using the LbL assembly approach and the novel polyanion **P2** possessing amphiphilic perfluoroalkyl and polyethylene glycol (fPEG) segments is proposed. With this method, it is possible to make PEG/fluorinated thin films in a fairly simple way, and with a high degree of control over the film thickness. Surface rearrangement of the polymeric film surface was studied with AFM and XPS. The AFM image of **F3** indicated a rough surface formed through thermodynamically induced process of mutual incompatibility. In addition, the XPS spectrum of **F3** showed concentrated fluorinated side groups on the surface. Observed contact angles for different liquids suggest the presence of a dynamic amphiphilic surface with ability for environmentally dependent surface reconstruction. The amphiphilic film showed reduced adhesion of a marine sourced bacterium (*Pseudomonas*, NCIMB 2021) and some reduction in microalgal slime formation. The proposed method may serve as an efficient approach to prepare stable and versatile marine antifouling coatings with controlled thickness, and further studies may be conducted to enhance the material's antifouling performance against microalgae. More antifouling assays such as cyprids settlement and raft assay may be applied to further evaluate the efficacy of the amphiphilic LbL films.

■ ASSOCIATED CONTENT

Supporting Information

ImageJ examples. FTIR and NMR spectra. DLS results. This material is available free of charge via the Internet at http://pubs.acs.org.

■ AUTHOR INFORMATION

Corresponding Authors

*Tel: +65 6874 5443; Fax: +65 6872 0785; E-mail: janczewskid@imre.a-star.edu.sg (D.J.).

*Tel: +31 53 489 2974; Fax: +31 53 489 3823; E-mail: g.j.vancso@utwente.nl (G.J.V.).

Notes

The authors declare no competing financial interest.

■ ACKNOWLEDGMENTS

The authors are grateful to the Agency for Science, Technology and Research (A*STAR) for providing financial support under the Innovative Marine Antifouling Solutions (IMAS) program.

■ REFERENCES

(1) Callow, J. A.; Callow, M. E. Trends in the development of environmentally friendly fouling-resistant marine coatings. *Nat. Commun.* **2011**, *2*, 244.

(2) Lejars, M.; Margaillan, A.; Bressy, C. Fouling release coatings: A nontoxic alternative to biocidal antifouling coatings. *Chem. Rev.* **2012**, *112* (8), 4347−4390.

(3) Salta, M.; Wharton, J. A.; Stoodley, P.; Dennington, S. P.; Goodes, L. R.; Werwinski, S.; Mart, U.; Wood, R. J. K.; Stokes, K. R. Designing biomimetic antifouling surfaces. *Philos. Trans. R. Soc. A* **2010**, *368* (1929), 4729−4754.

(4) Schultz, M. P.; Bendick, J. A.; Holm, E. R.; Hertel, W. M. Economic impact of biofouling on a naval surface ship. *Biofouling* **2011**, *27* (1), 87−98.

(5) Krishnan, S.; Weinman, C. J.; Ober, C. K. Advances in polymers for anti-biofouling surfaces. *J. Mater. Chem.* **2008**, *18* (29), 3405−3413.

(6) Schumacher, J. F.; Carman, M. L.; Estes, T. G.; Feinberg, A. W.; Wilson, L. H.; Callow, M. E.; Callow, J. A.; Finlay, J. A.; Brennan, A. B. Engineered antifouling microtopographies-effect of feature size, geometry, and roughness on settlement of zoospores of the green alga *Ulva*. *Biofouling* **2007**, *23* (1), 55−62.

(7) Schumacher, J. F.; Long, C. J.; Callow, M. E.; Finlay, J. A.; Callow, J. A.; Brennan, A. B. Engineered nanoforce gradients for inhibition of settlement (attachment) of swimming algal spores. *Langmuir* **2008**, *24* (9), 4931−4937.

(8) Verran, J.; Boyd, R. D. The relationship between substratum surface roughness and microbiological and organic soiling: A review. *Biofouling* **2001**, *17* (1), 59−71.

(9) Lindner, E. A low surface free energy approach in the control of marine biofouling. *Biofouling* **1992**, *6* (2), 193−205.

(10) Yang, W. J.; Neoh, K. G.; Kang, E. T.; Lee, S. S. C.; Teo, S. L. M.; Rittschof, D. Functional polymer brushes via surface-initiated atom transfer radical graft polymerization for combating marine biofouling. *Biofouling* **2012**, *28* (9), 895−912.

(11) Finlay, J. A.; Bennett, S. M.; Brewer, L. H.; Sokolova, A.; Clay, G.; Gunari, N.; Meyer, A. E.; Walker, G. C.; Wendt, D. E.; Callow, M. E.; Callow, J. A.; Detty, M. R. Barnacle settlement and the adhesion of protein and diatom microfouling to xerogel films with varying surface energy and water wettability. *Biofouling* **2010**, *26* (6), 657−666.

(12) Petrone, L.; Di Fino, A.; Aldred, N.; Sukkaew, P.; Ederth, T.; Clare, A. S.; Liedberg, B. Effects of surface charge and Gibbs surface

energy on the settlement behaviour of barnacle cyprids (*Balanus amphitrite*). *Biofouling* **2011**, *27* (9), 1043−1055.
(13) Chen, S.; Li, L.; Zhao, C.; Zheng, J. Surface hydration: Principles and applications toward low-fouling/nonfouling biomaterials. *Polymer* **2010**, *51* (23), 5283−5293.
(14) Quintana, R.; Gosa, M.; Jańczewski, D.; Kutnyanszky, E.; Vancso, G. J. Enhanced stability of low fouling zwitterionic polymer brushes in seawater with diblock architecture. *Langmuir* **2013**, *29* (34), 10859−10867.
(15) Cortez, C.; Quinn, J. F.; Hao, X.; Gudipati, C. S.; Stenzel, M. H.; Davis, T. P.; Caruso, F. Multilayer buildup and biofouling characteristics of PSS-*b*-PEG containing films. *Langmuir* **2010**, *26* (12), 9720−9727.
(16) Zhu, X.; Loo, H.-E.; Bai, R. A novel membrane showing both hydrophilic and oleophobic surface properties and its non-fouling performances for potential water treatment applications. *J. Membr. Sci.* **2013**, *436*, 47−56.
(17) Yebra, D. M.; Kiil, S.; Dam-Johansen, K. Antifouling technology - Past, present and future steps towards efficient and environmentally friendly antifouling coatings. *Prog. Org. Coat.* **2004**, *50* (2), 75−104.
(18) Brady, R. F. Properties which influence marine fouling resistance in polymers containing silicon and fluorine. *Prog. Org. Coat.* **1999**, *35* (1−4), 31−35.
(19) Sommer, S.; Ekin, A.; Webster, D. C.; Stafslien, S. J.; Daniels, J.; VanderWal, L. J.; Thompson, S. E. M.; Callow, M. E.; Callow, J. A. A preliminary study on the properties and fouling-release performance of siloxane−polyurethane coatings prepared from poly(dimethylsiloxane) (PDMS) macromers. *Biofouling* **2010**, *26* (8), 961−972.
(20) Statz, A.; Finlay, J.; Dalsin, J.; Callow, M.; Callow, J. A.; Messersmith, P. B. Algal antifouling and fouling-release properties of metal surfaces coated with a polymer inspired by marine mussels. *Biofouling* **2006**, *22* (6), 391−399.
(21) Krishnan, S.; Wang, N.; Ober, C. K.; Finlay, J. A.; Callow, M. E.; Callow, J. A.; Hexemer, A.; Sohn, K. E.; Kramer, E. J.; Fischer, D. A. Comparison of the fouling release properties of hydrophobic fluorinated and hydrophilic PEGylated block copolymer surfaces: Attachment strength of the diatom Navicula and the green alga *Ulva*. *Biomacromolecules* **2006**, *7* (5), 1449−1462.
(22) Youngblood, J. P.; Andruzzi, L.; Ober, C. K.; Hexemer, A.; Kramer, E. J.; Callow, J. A.; Finlay, J. A.; Callow, M. E. Coatings based on side-chain ether-linked poly(ethylene glycol) and fluorocarbon polymers for the control of marine biofouling. *Biofouling* **2003**, *19*, 91−98.
(23) Krishnan, S.; Ayothi, R.; Hexemer, A.; Finlay, J. A.; Sohn, K. E.; Perry, R.; Ober, C. K.; Kramer, E. J.; Callow, M. E.; Callow, J. A.; Fischer, D. A. Anti-biofouling properties of comblike block copolymers with amphiphilic side chains. *Langmuir* **2006**, *22* (11), 5075−5086.
(24) Martinelli, E.; Agostini, S.; Galli, G.; Chiellini, E.; Glisenti, A.; Pettitt, M. E.; Callow, M. E.; Callow, J. A.; Graf, K.; Bartels, F. W. Nanostructured films of amphiphilic fluorinated block copolymers for fouling release application. *Langmuir* **2008**, *24* (22), 13138−13147.
(25) Weinman, C. J.; Finlay, J. A.; Park, D.; Paik, M. Y.; Krishnan, S.; Sundaram, H. S.; Dimitriou, M.; Sohn, K. E.; Callow, M. E.; Callow, J. A.; Handlin, D. L.; Willis, C. L.; Kramer, E. J.; Ober, C. K. ABC triblock surface active block copolymer with grafted ethoxylated fluoroalkyl amphiphilic side chains for marine antifouling/fouling-release applications. *Langmuir* **2009**, *25* (20), 12266−12274.
(26) Kristalyn, C. B.; Lu, X.; Weinman, C. J.; Ober, C. K.; Kramer, E. J.; Chen, Z. Surface structures of an amphiphilic tri-block copolymer in air and in water probed using sum frequency generation vibrational spectroscopy. *Langmuir* **2010**, *26* (13), 11337−11343.
(27) Park, D.; Weinman, C. J.; Finlay, J. A.; Fletcher, B. R.; Paik, M. Y.; Sundaram, H. S.; Dimitriou, M. D.; Sohn, K. E.; Callow, M. E.; Callow, J. A.; Handlin, D. L.; Willis, C. L.; Fischer, D. A.; Kramer, E. J.; Ober, C. K. Amphiphilic surface active triblock copolymers with mixed hydrophobic and hydrophilic side chains for tuned marine fouling-release properties. *Langmuir* **2010**, *26* (12), 9772−9781.
(28) Tan, B. H.; Hussain, H.; Chaw, K. C.; Dickinson, G. H.; Gudipati, C. S.; Birch, W. R.; Teo, S. L. M.; He, C.; Liu, Y.; Davis, T. P. Barnacle repellent nanostructured surfaces formed by the self-assembly of amphiphilic block copolymers. *Polym. Chem.* **2010**, *1* (3), 276−279.
(29) Feng, S.; Huang, Y.; Wang, Q.; Qing, F.-L. Nonbiofouling surface based on amphiphilic alkanethiol self-assembled monolayers. *Surf. Interface Anal.* **2011**, *43* (4), 770−776.
(30) Wang, Y.; Betts, D. E.; Finlay, J. A.; Brewer, L.; Callow, M. E.; Callow, J. A.; Wendt, D. E.; DeSimone, J. M. Photocurable amphiphilic perfluoropolyether/poly(ethylene glycol) networks for fouling-release coatings. *Macromolecules* **2011**, *44* (4), 878−885.
(31) Wang, Y.; Pitet, L. M.; Finlay, J. A.; Brewer, L. H.; Cone, G.; Betts, D. E.; Callow, M. E.; Callow, J. A.; Wendt, D. E.; Hillmyer, M. A.; DeSimone, J. M. Investigation of the role of hydrophilic chain length in amphiphilic perfluoropolyether/poly(ethylene glycol) networks: Towards high-performance antifouling coatings. *Biofouling* **2011**, *27* (10), 1139−1150.
(32) Joshi, R. G.; Goel, A.; Mannari, V. M.; Finlay, J. A.; Callow, M. E.; Callow, J. A. Evaluating fouling-resistance and fouling-release performance of smart polyurethane surfaces: An outlook for efficient and environmentally benign marine coatings. *J. Appl. Polym. Sci.* **2009**, *114* (6), 3693−3703.
(33) Gudipati, C. S.; Greenlief, C. M.; Johnson, J. A.; Prayongpan, P.; Wooley, K. L. Hyperbranched fluoropolymer and linear poly(ethylene glycol) based Amphiphilic crosslinked networks as efficient antifouling coatings: An insight into the surface compositions, topographies, and morphologies. *J. Polym. Sci. A: Polym. Chem.* **2004**, *42* (24), 6193−6208.
(34) Gudipati, C. S.; Finlay, J. A.; Callow, J. A.; Callow, M. E.; Wooley, K. L. The antifouling and fouling-release perfomance of hyperbranched fluoropolymer (HBFP)−poly(ethylene glycol) (PEG) composite coatings evaluated by adsorption of biomacromolecules and the green fouling alga *Ulva*. *Langmuir* **2005**, *21* (7), 3044−3053.
(35) Imbesi, P. M.; Gohad, N. V.; Eller, M. J.; Orihuela, B.; Rittschof, D.; Schweikert, E. A.; Mount, A. S.; Wooley, K. L. Noradrenaline-functionalized hyperbranched fluoropolymer−poly(ethylene glycol) cross-linked networks as dual-mode, anti-biofouling coatings. *ACS Nano* **2012**, *6* (2), 1503−1512.
(36) Izquierdo, A.; Ono, S. S.; Voegel, J. C.; Schaaf, P.; Decher, G. Dipping versus spraying: Exploring the deposition conditions for speeding up layer-by-layer assembly. *Langmuir* **2005**, *21* (16), 7558−7567.
(37) Ma, Y.; Dong, W. F.; Hempenius, M. A.; Möhwald, H.; Vancso, G. J. Redox-controlled molecular permeability of composite-wall microcapsules. *Nat. Mater.* **2006**, *5* (9), 724−729.
(38) Song, J.; Jańczewski, D.; Ma, Y.; van Ingen, L.; Ee Sim, C.; Goh, Q.; Xu, J.; Vancso, G. J. Electrochemically controlled release of molecular guests from redox responsive polymeric multilayers and devices. *Eur. Polym. J.* **2013**, *49* (9), 2477−2484.
(39) Lichter, J. A.; Rubner, M. F. Polyelectrolyte multilayers with intrinsic antimicrobial functionality: The importance of mobile polycations. *Langmuir* **2009**, *25* (13), 7686−7694.
(40) Kuo, W. H.; Wang, M. J.; Chien, H. W.; Wei, T. C.; Lee, C.; Tsai, W. B. Surface modification with poly(sulfobetaine methacrylate-*co*-acrylic acid) to reduce fibrinogen adsorption, platelet adhesion, and plasma coagulation. *Biomacromolecules* **2011**, *12* (12), 4348−4356.
(41) Zhu, X.; Jańczewski, D.; Lee, S. S. C.; Teo, S. L. M.; Vancso, G. J. Cross-linked polyelectrolyte multilayers for marine antifouling applications. *ACS Appl. Mater. Interfaces* **2013**, *5* (13), 5961−5968.
(42) Yang, W. J.; Pranantyo, D.; Neoh, K. G.; Kang, E. T.; Teo, S. L. M.; Rittschof, D. Layer-by-layer click deposition of functional polymer coatings for combating marine biofouling. *Biomacromolecules* **2012**, *13* (9), 2769−80.
(43) Cao, X.; Pettitt, M. E.; Wode, F.; Arpa Sancet, M. P.; Fu, J.; Ji, J.; Callow, M. E.; Callow, J. A.; Rosenhahn, A.; Grunze, M. Interaction of zoospores of the green alga *Ulva* with bioinspired micro- and nanostructured surfaces prepared by polyelectrolyte layer-by-layer self-assembly. *Adv. Funct. Mater.* **2010**, *20* (12), 1984−1993.
(44) Liu, T.; Yin, B.; He, T.; Guo, N.; Dong, L.; Yin, Y. Complementary effects of nanosilver and superhydrophobic coatings

on the prevention of marine bacterial adhesion. *ACS Appl. Mater. Interfaces* **2012**, *4* (9), 4683−4690.
(45) Rasmussen, K.; Østgaard, K. Adhesion of the marine fouling diatom amphora coffeaeformis to non-solid gel surfaces. *Biofouling* **2001**, *17* (2), 103−115.
(46) Al-Tahhan, R. A.; Sandrin, T. R.; Bodour, A. A.; Maier, R. M. Rhamnolipid-induced removal of lipopolysaccharide from *Pseudomonas aeruginosa*: Effect on cell surface properties and interaction with hydrophobic substrates. *Appl. Environ. Microbiol.* **2000**, *66* (8), 3262−3268.
(47) Lefaux, C. J.; Zimberlin, J. A.; Dobrynin, A. V.; Mather, P. T. Polyelectrolyte spin assembly: Influence of ionic strength on the growth of multilayered thin films. *J. Polym. Sci., Part B: Polym. Phys.* **2004**, *42* (19), 3654−3666.
(48) Yuan, S. J.; Pehkonen, S. O. Microbiologically influenced corrosion of 304 stainless steel by aerobic *Pseudomonas* NCIMB 2021 bacteria: AFM and XPS study. *Colloids Surf., B* **2007**, *59* (1), 87−99.
(49) Holland, R.; Dugdale, T. M.; Wetherbee, R.; Brennan, A. B.; Finlay, J. A.; Callow, J. A.; Callow, M. E. Adhesion and motility of fouling diatoms on a silicone elastomer. *Biofouling* **2004**, *20* (6), 323−329.
(50) Guillard, R. R.; Ryther, J. H. Studies of marine planktonic diatoms 0.1. Cyclotella nana Hustedt, and Detonula confervacea (Cleve) Gran. *Can. J. Microbiol.* **1962**, *8* (2), 229−239.
(51) Martinelli, E.; Menghetti, S.; Galli, G.; Glisenti, A.; Krishnan, S.; Paik, M. Y.; Ober, C. K.; Smilgies, D.-M.; Fischer, D. A. Surface engineering of styrene/PEGylated-fluoroalkyl styrene block copolymer thin films. *J. Polym. Sci. A: Polym. Chem.* **2009**, *47* (1), 267−284.
(52) Pretsch, E.; Bnhlmann, P.; Affolter, C. *Structure Determination of Organic Compounds*; Springer: Berlin/Heidelberg, 2009.
(53) Ma, N.; Zhang, H. Y.; Song, B.; Wang, Z. Q.; Zhang, X. Polymer micelles as building blocks for layer-by-layer assembly: An approach for incorporation and controlled release of water-insoluble dyes. *Chem. Mater.* **2005**, *17* (20), 5065−5069.
(54) Ma, N.; Wang, Y. P.; Wang, Z. Q.; Zhang, X. Polymer micelles as building blocks for the incorporation of azobenzene: Enhancing the photochromic properties in layer-by-layer films. *Langmuir* **2006**, *22* (8), 3906−3909.
(55) von Klitzing, R. Internal structure of polyelectrolyte multilayer assemblies. *Phys. Chem. Chem. Phys.* **2006**, *8* (43), 5012−5033.
(56) Park, D.; Keszler, B.; Galiatsatos, V.; Kennedy, J. P.; Ratner, B. D. Amphiphilic networks 0.9. Surface characterization. *Macromolecules* **1995**, *28* (8), 2595−2601.
(57) Howarter, J. A.; Youngblood, J. P. Self-cleaning and anti-fog surfaces via stimuli-responsive polymer brushes. *Adv. Mater.* **2007**, *19* (22), 3838−3843.
(58) Howarter, J. A.; Youngblood, J. P. Amphiphile grafted membranes for the separation of oil-in-water dispersions. *J. Colloid Interface Sci.* **2009**, *329* (1), 127−132.
(59) Pang, C. M.; Hong, P. Y.; Guo, H. L.; Liu, W. T. Biofilm formation characteristics of bacterial isolates retrieved from a reverse osmosis membrane. *Environ. Sci. Technol.* **2005**, *39* (19), 7541−7550.
(60) Lee, S. Y.; Kim, H. J.; Patel, R.; Im, S. J.; Kim, J. H.; Min, B. R. Silver nanoparticles immobilized on thin film composite polyamide membrane: characterization, nanofiltration, antifouling properties. *Polym. Adv. Technol.* **2007**, *18* (7), 562−568.